EBioMedicine 53 (2020) 102696

Contents lists available at ScienceDirect

EBioMedicine

journal homepage: www.elsevier.com/locate/ebiom

Research paper

Enhanced monoacylglycerol lipolysis by ABHD6 promotes NSCLC pathogenesis

Zhiyuan Tang[a,b,1], Hao Xie[c,1], Christoph Heier[c], Jianfei Huang[d], Qiuling Zheng[b], Thomas O. Eichmann[c,e], Gabriele Schoiswohl[c], Jun Ni[f], Rudolf Zechner[c], Songshi Ni[g,*], Haiping Hao[b,*]

[a] Department of Pharmacy, Affiliated Hospital of Nantong University, Nantong 226001, China
[b] Key Laboratory of Drug Metabolism and Pharmacokinetics, State Key Laboratory of Natural Medicines, China Pharmaceutical University, Nanjing, Jiangsu 210009, China
[c] Institute of Molecular Biosciences, University of Graz, Graz 8010, Austria
[d] Department of Clinical Biobank, Affiliated Hospital of Nantong University, Nantong 226001, China
[e] Center for Explorative Lipidomics, BioTechMed-Graz, Graz 8010, Austria
[f] Department of Rehabilitation, The First Affiliated Hospital of Fujian Medical University, Fujian 350000, China
[g] Department of Respiratory and Critical Care Medicine, Affiliated Hospital of Nantong University, Nantong 226001, China

ARTICLE INFO

Article History:
Received 16 September 2019
Revised 14 February 2020
Accepted 14 February 2020
Available online xxx

Keywords:
NSCLC
ABHD6
Aggressiveness
MAG

ABSTRACT

Background: Tumor cells display metabolic changes that correlate with malignancy, including an elevated hydrolysis of monoacylglycerol (MAG) in various cancer types. However, evidence is absent for the relationship between MAG lipolysis and NSCLC.

Methods: MAG hydrolase activity assay, migration, invasion, proliferation, lipids quantification, and transactivation assays were performed in vitro. Tumor xenograft studies and lung metastasis assays were examined in vivo. The correlations of MAGL/ABHD6 expression in cancerous tissues with the clinicopathological characteristics and survival of NSCLC patients were validated.

Findings: ABHD6 functions as the primary MAG lipase and an oncogene in NSCLC. MAG hydrolase activities were more than 11-fold higher in cancerous lung tissues than in paired non-cancerous tissues derived from NSCLC patients. ABHD6, instead of MAGL, was significantly associated with advanced tumor node metastasis (TNM) stage (HR, 1.382; P = 0.004) and had a negative impact on the overall survival of NSCLC patients (P = 0.001). ABHD6 silencing reduced migration and invasion of NSCLC cells in vitro as well as metastatic seeding and tumor growth in vivo. Conversely, ectopic overexpression of ABHD6 provoked the pathogenic potential. ABHD6 blockade significantly induced intracellular MAG accumulation which activated PPARα/γ signaling and inhibited cancer pathophysiology.

Interpretation: The present study provide evidence for a previously uncovered pro-oncogenic function of ABHD6 in NSCLC, with the outlined metabolic mechanisms shedding light on new potential strategies for anticancer therapy.

Fund: This work was supported by the Project for Major New Drug Innovation and Development (2015ZX09501010 and 2018ZX09711001-002-003).

1. Introduction

Malignant transformation, the progression of cells from a normal to cancerous state, requires the reprogramming of numerous metabolic pathways. The most commonly observed metabolic alteration in cancer is enhanced glycolysis [1]. Other metabolic adaptations of cancer cells include increased rates of glutamine metabolism and elevated fatty acids (FAs) synthesis [2–4]. More recent studies implicate that cancer cells require increased MAG lipolysis catalyzed by monoacylglycerol lipase (MAGL) to promote cancer pathophysiology, including melanoma, ovarian, breast, prostate, nasopharyngeal, and hepatic cancers [5–9]. Mechanistically, MAGL regulates malignancy through a tumor-promoting FA network in cancer cells from multiple tissues of origin and 2-arachidonoylglycerol (2-AG) mediated endocannabinoid system in prostate cancer cells [7].

* Corresponding authors.
E-mail addresses: jsntnss@163.com (S. Ni), haipinghao@cpu.edu.cn (H. Hao).
[1] These authors contributed equally to this work.

https://doi.org/10.1016/j.ebiom.2020.102696

Research in context

Evidence before this study

Abnormal lipid metabolism underlies chronic pathologies such as obesity, diabetes, and cancer. Recently, accumulating evidence suggests that enhanced hydrolysis of monoacylglycerol (MAG) catalyzed by monoacylglycerol lipase (MAGL) is a common pathological event in many types of cancer cells. However, critical questions remained unanswered in terms of MAG catabolism in malignancy, particularly in the context of lung cancer. Moreover, potential roles of other MAG lipases are poorly described in cancer biology.

Added value of this study

Our findings from cell, animal, and human studies support that α/β-hydrolase domain-containing 6 (ABHD6) functions as the predominant MAG lipase and an important oncogene in NSCLC. ABHD6 catabolizes saturated and monounsaturated MAG species rather than 2-arachidonoylglycerol (2-AG) to augment NSCLC pathogenesis.

Implications of all the available evidence

Our work suggests that ABHD6 has significant potential as diagnostic marker and therapeutic target for the treatment of NSCLC.

NSCLC, which accounts for more than 80% of lung cancer patients, represents the most common malignancy and the leading cause of cancer deaths in America [10]. Whether and how MAG catabolism is implicated in NSCLC remains largely unexplored. In an activity-based assay, we found that MAG hydrolase activity was significantly enhanced in cancerous tissues as compared to adjacent non-cancerous tissues derived from NSCLC patients. Since MAGL is expressed at low levels in NSCLC cells contributing little to intracellular MAG hydrolase activity, we explored whether and how other MAG lipases are involved in NSCLC.

Besides MAGL, MAG can be hydrolyzed by α/β-hydrolase domain-containing 6 (ABHD6), with its catalytic site facing the cytosol and ABHD12 with exterior facing catalytic site [11]. Recent studies suggested a potential role of ABHD6 in MAG hydrolysis of pancreatic β cells, macrophages, neurons, and white adipocytes and has been associated with insulin secretion, inflammation, neurotransmission, the central control of energy homeostasis, and adipose tissue browning [12–16]. However, current knowledge about the malignant function of ABHD6 remains unclear despite high mRNA levels of ABHD6 are observed in certain cancer cell lines [17,18].

Here, we show that ABHD6 is the primary MAG lipase in NSCLC. ABHD6 silencing limits the development of NSCLC by suppressing migration, invasion, metastasis, and in vivo tumor growth. ABHD6 blockade fails to affect endocannabinoids system, but significantly induces intracellular MAG accumulation which inhibits cancer pathophysiology and activates PPARα/γ signaling. The finding that high expression of ABHD6 is associated with advanced tumor-node-metastasis (TNM) stage and worse prognosis in patients with NSCLC adds important clinical relevance to this work.

2. Methods

2.1. Patients and tumor specimens

In this study, 206 patients with NSCLC were invited to participate in this research with formalin-fixed and paraffin-embedded cancerous and matched neighboring non-cancerous tissues whose number were 206 and 102 respectively. This patient group consists of 49 women and 157 men, whose ages varied from 37 to 83 years old. Their clinical characteristics that we got were mainly from their corresponding medical records. Also, before surgery, it was ensured that none of these patients had ever received treatments such as neoadjuvant chemotherapy, radiotherapy or immunotherapy. The pathology staff transported the surgical removal tissue samples to the clinical biobank for further study in 15 min. We froze the samples and measured the activity in a trial to ensure homogeneity and validity of the results.

2.2. Cell lines

NSCLC cell lines A549, SPC-A-1, NCI-H1675, and NCI-H1650 were obtained from the Cell Bank, Type Culture Collection, Chinese Academy of Science (CBTCCCAS, Shanghai, China). NSCLC cells were maintained in RPMI 1640 medium (Invitrogen). All media were supplemented with 10% FBS (Thermo Fisher), 1% penicillin/streptomycine. INS-1 cells was maintained in RPMI 1640 medium containing 11.1 mM D-glucose with addition of 10% FBS, 10 mM HEPES, 1% penicillin/streptomycine, 1 mM sodium pyruvate, and 50 μM β-mercaptoethanol. All cells were cultured at 37 °C in a 5% CO_2 humidified atmosphere.

2.3. Experimental animals

4-week-old male BALB/c-nude mice and 7-week-old NOD/SCID mice were purchased from Shanghai Experimental Animal Center (Shanghai, China). All mice were raised in a pathogen-free environment and fed a normal chow and water ad libitum.

2.4. Cell culture, reagents, RNA interference, and transfection

The negative control duplex (named shControl, sense: 5′-TTCTCCGAACGTGTCACGT-3′) without any significant sequence homology with apprehended gene and three small interfering RNA targeting human ABHD6 mRNA (called shABHD6, shRNA-1 sense: 5′-CAGCCAAGCTCATAATCGA-3′; shRNA-2 sense: 5′-GCCAAGTCAATTGCCAACT-3′; shRNA-3 sense: 5′-GCAGTACTCAACTGACAAT-3′) were applied for purpose of this research of lose-of-function. Among the sequences with the highest efficiency, shRNA-1 by Quantitative real time polymerase chain reaction (Q-PCR) and western blot analysis were applied. The shControl sequence as well as shRNA-1 sequence was connected with pRNAU6.1/NEO vector, into which the full-length ABHD6 cDNA was cloned. GFP tested and screened the cell lines with plasmids. The medium containing 200 μg/ml G418 (Invitrogen) was developed for cultivating the cells. Q-PCR is utilized to prove the plasmid expressions. After a period of 30 days, cell clones were then isolated and further replicated. ABHD6 stably silenced cell lines were generated and named shABHD6 A549, shABHD6 SPC-A-1 respectively. And cells transfected by the negative control vector were named shControl. The cDNA encoding the full-length human ABHD6 (NM_001320126) was amplified by Q-PCR and cloned in the expression vector pTracer-CMV2. Then we screened with zeocin to generate H1975 and H1650 cells stably overexpressing ABHD6 protein. And the cells were named H1975 OE and H1650 OE. Empty vector transfected group was served as control. Small interfering RNA targeting MAGL, ABHD6, and ABHD12 were also applied for the MAG hydrolase activity measurements.

2.5. MAG hydrolase activity measurements

Tissue samples were made homogenized by means of solution B (0.25 M sucrose; 1 mM EDTA; 20 μM DTT pH 7.0 with acetic acid; 2 μg/ml antipain; 20 μg/ml leupeptin; 1 μg/ml pepstatin as protease inhibitor) on ice and further centrifuged at 1000 g, at the temperature of 4 °C for 10 min in total. Then by transferring to a new tube, the supernatant was centrifuged at 20,000 g at 4 °C for 30 min. The infranatant was carefully

collected by a hot needle, leaving the upper layer. MAG hydrolase activity is determined on the 20,000 g infranatant.

Cultured cells (5×10^6) were harvested and disrupted in 200 μl solution B by sonication. Then cell extracts were made centrifuged at 1000 g, 4 °C for 10 min, which was further used to measure MAG hydrolase activity. Add 1 mM lipid substrate (C16:0 MAG or C18:1 MAG) and dry it completely under a stream of nitrogen. Add 0.1 M potassium phosphate buffer (pH 7.0) and sonicate on ice for 10 s per ml of substrate. Then FA-free BSA was added with the substrate in an equimolar ratio. Add 20% BSA and sonicate for 5 secs to obtain a clear substrate solution. Then 10 μl of sample in solution B was prepared in 1.5 ml tube, and 100 μl solution B was used as blank. And substrate with final the concentration 100 μM was added, which were incubated at 37 °C for 30 min under continuous shaking (300−500 rpm/min). After adding 100 μl chloroform, the reaction was terminated. They were put into vigorous vortex for 10 s, and served for the later phase separation by being centrifuged at 10,000 g for 2 min. 50 μl of the upper phase (aqueous phase) was then diverted into a 96-well plate. Free Glycerol Reagent was used for the detection and a 562 nm filter was applied to obtain the readings with 96-well plate reader.

2.6. Immunoblotting

Cells were lysed by Lysis buffer, and then the BSA method was applied to decide following transfection and protein concentration. A 10% SDS-polyacrylamide gels was used to separate equivalent quantities of protein, which were then transferred to Polyvinylidene Fluoride Membrane. 5% non-fat milk was utilized to block membranes, and then the proper primary antibody was applied for the overnight incubation. Cells were washed with TBST for three times and a secondary antibody conjugated with HRP was utilized at the dilution of 1:5000 for 1 h at indoor temperature. Primary immunoblotting antibodies included anti-S100A4 (Cat. No. ab124805, Abcam, dilution 1:1000, RRID: AB_10978091), anti-E-caderin (Cat. No. ab1416, Abcam, dilution 1:1000, RRID: AB_300946), anti-Vimentin (Cat. No. ab92547, Abcam, dilution 1:1000, RRID: AB_10562134), anti-SNAIL (Cat. No.31787, Abcam, dilution 1:1000, RRID: AB_1281121), anti-ABHD6 (Cat. No. ab 230423, Abcam, dilution 1:1000, RRID: AB_1523059), anti-MAGL (Cat. No. ab 24701, Abcam, dilution 1:1000, RRID: AB_448238), anti-ABHD12(Cat. No. ab87048, abcam, dilution 1:1000, RRID: AB_1951393), anti-β-Actin (Cat. No. 4970, Cell Signaling, dilution 1:1000, RRID: AB_2223172).

2.7. Measurement of lipid in tissues and cancer cells

Cell metabolites or tissues in a total volume of 250 μl water were extracted in 1.4 ml solution which was a 2:1:1 mixture of chloroform: water: methanol. Samples were made into homoenates in accordance with internal standards (including PC-14:0/14:0, PE-14:0/14:0, PS-34:1/d31, PA-17:0/17:0, PG-14:0/14:0, PI-34:1/d31, LPC—C17:0, LPE-C17:0, MAG-C17:0, etc.) and then centrifuged at 18,000 rpm for 10 min. Turn to the bottom phase to the tube, which was dried under the condition of N_2 and then dissolved in 100 μl acetonitrile. Centrifuge the samples at 18,000 rpm for 10 min and LC-MS is made use of in the analysis of 50 μl of the samples. With the use of BCA protein assay Kit (Beyotime Institute of Biotechnology), the data of the total concentrations of cytosolic proteins in cell and tissue samples were obtained.

LC-MS analysis was carried out by means of an instrument named Waters Synapt G2-Si QTOF-MS. Separation of individual polar lipids would be carried out using a Phenomenex Luna 3 μm silica column (i.d. 150 × 2.0 mm) with the following conditions: mobile phase A (chloroform:methanol:ammonium hydroxide, 89.5:10:0.5), B (chloroform:methanol:ammonium hydroxide:water, 55:39:0.5:5.5). Glycerol lipids were analyzed using a modified version of reverse phase HPLC/ESI/MS [19]. Separation of lipids aforementioned was carried out on a Phenomenex Kinetex 2.6 μm-C18 column (i.d. 4.6 × 100 mm) using an isocratic mobile phase chloroform: methanol:0.1 M ammonium acetate (100:100:4) at a flow rate of 150 μl/min for 17 min. The data obtained through UPLC-QTOF-MS were subjected to QuanLynx applications manager version for the purpose of detecting peak signals, obtaining calibration equations, and calculating the concentration of each metabolite. Manual examination and correction were of absolute necessity in order to ensure the quality of the data.

2.8. Drug treatment for cancer cells

To maintain NSCLC cancer cells, RPMI 1640 medium containing 10% (v/v) fetal bovine serum (FBS) was applied. A hemocytometer was used to trypsinize and count cells. A total of 24 h after plating, serum-free medium took place of the complete medium for 24 h. Cells were cultivated in the medium named serum-free RPMI 1640 with JZL184 (Selleck) (1 μM, 8 h), WWL70 (Sigma) (10 μM, 8 h), KT203 (APExBIO) (10 nM, 8 h), AM251 (Medchemexpress) (50 nM, 8 h), AM630 (Medchemexpress) (50 nM, 8 h), GW6471 (Sigma) (1 μM, 8 h), T0070907 (Selleck) (1 μM, 8 h), Arachidonic acid (AA) (Sigma) (50 μM, 8 h), C16:0 MAG (5 nM, 10 nM, 100 nM, 1 μM, 5 μM, 10 μM, 8 h, add FA-free BSA to give a final concentration of 1%), C18:1 MAG (5 nM, 10 nM, 100 nM, 1 μM, 5 μM, 10 μM, 8 h, add FA-free BSA to give a final concentration of 1%), C16:0 FA (5 nM, 10 nM, 100 nM, 1 μM, 5 μM, 8 h), C18:1 FA (5 nM, 10 nM, 100 nM, 1 μM, 5 μM, 8 h) or vehicle (DMSO) at 0.1%. For cells of shControl or shABHD6 groups, the medication time was same. Cells were harvested for migration and invasion or other further assays. To avoid lipotoxicity from FA overload, we examined whether BSA supplementation affect our migration study or not. The conjugation of FAs to 1% BSA did not show additional effect on cell migration.

2.9. Transwell migration and invasion assays

Cell migration and intrusion test was conducted in transwell chambers. In terms of the invasive experiment, Matrigel was utilized to pre-coat the inserts on the upper-surface. After transfection or drug treatment, cells (8×10^4) were temporarily kept in the medium of 0.2 ml serum-free medium and later seeded to the upper compartment. What's more, 0.6 ml medium with 10% FBS was put to the lower compartment and played the role of a chemo attractant. Cells were incubated at 37 °C, and 24 h later, a cotton swab was used to carefully remove the top layer of cells, and 4% paraformaldehyde was added to maintain cells of the lower surface and 0.3% trypan blue to stain. And the number of cells in five fields which were selected at random (total magnification, × 200) was obtained by counting under a light microscope for the assessment of cell migration and intrusion. For each replicate, the results were averaged and compared with controls.

2.10. Cell proliferation assay

The SPC-A-1, A549, H1975, and H1650 cells were seeded in each well with 3×10^3 cells in 100 μl of growth medium in a 96-well plate 24 h before the experiment. Remove the medium and wash cells twice by fresh medium. Then they were incubated with or without 10 μM WWL70 for 8 h. Four kinds of shABHD6 or shControl NSCLC cells were seeded at 3×10^3 cells in every well in 100 μl of growth medium. The medium was replaced with CCK-8 at every time point. After cells were cultured at the temperature of 37 °C for 1 h, the absorbance of 450 nm was obtained by a MRX II absorbance measurement.

2.11. In vivo tumor xenograft studies

Animal study was conducted under the condition of strictly following the institutional regulations for the care and use of animals. Each nude mouse was subcutaneously injected with shABHD6 A549, shControl A549, shABHD6 SPC-A-1, or shControl SPC-A-1 cells (1×10^7 in

100 μl PBS) at the right flank. In the parallel experiment nude mice were subcutaneously injected H1975 OE or H1650 OE cells. And we set up the control and parental group at the same time. Animals were monitored daily for physical well-being. When visible tumors were observed, two were measured by a caliper is used to measure the two perpendicular diameters every other two days, and the tumor volume was obtained by formula $V = \text{width}^2 \times \text{length} \times 0.52$. After 4 weeks, 10% formalin is used to fix the parts of tumors which later experienced the Immunohistochemical staining and examined by pathology staff. The left tumors were frozen at the temperature of −80 °C in order to carry out the following experiments.

2.12. Tumor xenograft mouse fed with PPAR α/γ antagonist

Nude mice were given food and water ad libitum under constant conditions (12:12 h light: dark cycle, 60% humidity at 22±2 °C) for two weeks. A549 and SPC-A-1 cell lines were applied in the animal experiment. Each cell line consisted of five sub-groups. There were five mice in each group. All mice were subcutaneously injected with 1×10^7 cells (suspended in 100 μl PBS) to right flank injection respectively. The inhibitor was given to the shABHD6 groups. GW6471 and T0070907 administration used in the experiment were conferred to 1 mg/kg body weight by oral gavage in polyethylene glycol 300. The dosing volume of the mixture group remained unchanged. The inhibitors were given every two days (at approximately the same time the day the inhibitor was given) for 35 days. The treatments were initiated immediately after injection of cancer cells. The groups which were untreated with inhibitors had normal diet. The model was totally of 7 weeks' duration.

2.13. Dietary AA for tumor xenograft mouse

A549 and SPC-A-1 cell lines were applied. Each cell line consisted of four sub-groups. There were five mice in each group. Mice were injected with the corresponding group of cells (1×10^7 in 100 μl PBS) at the right flank. AA (1.1 g/kg) was administrated every day (at approximately the same time the day) for 28 days. The drug untreated group had normal diet. Treatment began immediately after the injection of the cancer cells. The similar method was used to measure and calculate the volumes of tumor as described before.

2.14. Experimental lung metastasis assays

The cells from different groups (shControl A549, shABHD6 A549, shControl SPC-A-1, shABHD6 SPC-A-1 cells) were harvested from the flasks using trypsin. They were diluted with the medium, counted and resuspended in PBS after removal of the trypsin and medium to a final concentration of 10^6 cells/100 μl of PBS. 7-week-old NOD/SCID mice were injected with 0.2 ml suspension through the lateral tail vein. 2 days or 7 weeks later, all mice were sacrificed and lungs were removed. Four mice were used in one single experiment in one group. And we repeated this experiment twice. The long-term lung metastasis assay was also performed with NSCLC cells transfected with control or ABHD6-OE vectors. To assess proliferation in vivo, NOD/SCID mice were made injection of 10^7 cells from various groups in 200 μl PBS on the lateral tail vein. A 10 mg/ml solution of BrdU in DPBS is provided for in vivo use. And mice in each group were inoculated intraperitoneally with BrdU (50 mg/kg) in PBS per animal. After 48 h, lungs were harvested, cutting into pieces. Then the lungs were digested in a solution mixed with 10% collagenase IV (10 mg/ml in HBSS), 10% trypsin (0.25% in EDTA), and 10% dispase in HBSS without $Ca^{2+}$and Mg^{2+} at 37 °C for 1 h Digestion was terminated by RPMI 1640 Medium containing 10% FBS and DNase (5 mg/ml in HBSS). Then the suspension was then filtered and centrifuged through a 40 μm sieve. Then repeat the washing the filtering of the suspension in order to sort the samples for GFP positive cells. Cell sorting was conducted on BD FACS AriaTM cell sorters. And then cells were stained using the APC BrdU Flow Kit (BD Bioscience) in accordance with the manufacturer's protocol before experiencing analysis on a flow cytometer.

2.15. RNA extraction and quantitative real-time PCR (Q-PCR)

RNAiso Plus was used to extract the entire RNA, which was transferred into cDNA through reverse transcription with the application of the RevertAid First Strand cDNA Synthesis Kit (Thermo Fisher), and then Q-PCR was further carried out. PCR reaction mixtures containing 1 mg of cDNA were prepared using SYBR Green Master Mix with primers. After normalization of a reference GAPDH, which is also endogenous, the expressed gene levels were quantified by the $2^{-\Delta\Delta Ct}$ method. With the help of ABI 7500 FAST Real-Time PCR System, Q-PCR was successfully conducted. Primers used for Q-PCR are shown in Supplementary Table 2.

2.16. PPAR transactivation experiment

HEK-293T cells were transfected by the plasmids expressing PPAR, PPARβ or PPARγ, PPAR response element-directed luciferase expression plasmid (PPRE X3-TK-luc), and Renilla luciferase control plasmid. The transfected cells were kept for the entire night in FBS-free DMEM and were incubated for another 24 h in DMEM with 10 μM C18:1 MAG, 10 μM C16:0 MAG, or vehicle (DMSO) at 0.1% without FBS. Then, lysis cells and luciferase assays were performed. Renilla luciferase activity was used to standardize the expression of luciferase under PPRE guidance.

2.17. Immunohistochemical staining

IHC staining was independently evaluated and marked by two pathologists. Tissue microarrays from patients or mice were produced and samples of core tissues with 2 mm in diameter were gained from tissue sections which were embedded with paraffin and stored in paraffin-recipient blocks. In terms of antigen retrieval, sodium citrate buffer was utilized to heat slides for 3 min. The slides were blocked with Bovine Serum Albumin, and then the primary antibodies for anti-MAGL (dilution, 1:200), anti-ABHD6 (dilution, 1:100), anti-Vimentin (dilution, 1:200), anti-SNAIL (dilution, 1:250, Cat. No. ab 53519, Abcam, dilution 1:200, RRID: AB_881666), anti-S100A4 (dilution, 1:250), anti-E-caderin (dilution, 1:50), anti-CD34 (Cat. No. ab81289, dilution, 1:2500, RRID: AB_1640331), anti-VEGF (Cat. No. ab32152, Abcam, dilution, 1:250, RRID: AB_778798) were used to incubate the slides at 4 °C overnight. PBS was utilized to wash the slides three times, and then a HRP-conjugated secondary antibody was used to incubate at the indoor temperature for 60 min. For the purpose of staining, DAB solution was employed. The score ranges from 0 to 300 for the semi-quantification of positive strength, in which 0 means that none was stained while 300 means all were completely stained. And then the expression of protein was separated into two categories using the X-file software with a cut-off point 100, which referred to low expression and high expression.

2.18. Immunofluorescence

The cells were fixed by using 4% paraformaldehyde in PBS pH 7.4 for 10 min at room temperature. Then the cells were washed three times with ice-cold PBS. Incubate the samples for 10 min with PBS containing either 0.1−0.25% Triton X-100. Wash cells in PBS three times for 5 min. Incubate cells with 1% BSA, 22.52 mg/mL glycine in PBST (PBS+ 0.1% Tween 20) for 30 min to block unspecific binding of the antibodies. Incubate cells in the diluted antibody (anti-ABHD6 (Cat. No. ab 230423, Abcam, dilution 1:100), anti-MAGL (Cat. No. ab246902, Abcam, dilution 1:100)) in 1% BSA in PBST in a humidified chamber overnight at 4 °C. Decant the solution and wash the cells three times in PBS, 5 min each wash. Incubate cells with the secondary antibody in 1% BSA for 1 h at room temperature in the dark. Decant the secondary antibody solution and wash three times with

PBS for 5 min each in the dark. Mount coverslip with a drop of mounting medium. Seal coverslip with nail polish to prevent drying and movement under microscope.

2.19. Statistical analysis

Statistical analyses were performed in GraphPad Prism 7. We compared the differences in clinical features By means of the $\chi 2$ test. With Kaplan-Meier method along with log-rank test OS rates were easily calculated and the difference of OS rates of patients was clear. Also, the independent prognostic factors were obtained when multivariate analysis was combined with Cox regression analysis which adopted the proportional hazards model. For the cell and animal tests, two-sided student's *t*-test statistical analysis was performed for two groups. One-way ANOVA with Dunnett's test was performed for multiple comparisons with Specific comparisons between two groups.

2.20. Ethics statement

This study was officially recognized for it strictly carried out the procedures for care and use admitted by the Ethics Committee of the Affiliated Hospital of Nantong University (Ethic Number: 2018-K020). Written informed consent was obtained from each patient included in the study.

3. Results

3.1. High ABHD6 expression correlates positively with the poor prognosis of patients with NSCLC

To investigate the role of lipid catabolism and more specifically MAG hydrolysis in NSCLC, we first compared MAG hydrolase activities in homogenates of cancerous lung tissues and adjacent non-cancerous tissues from human patients. The homogenates of rat brain tissues, where MAGL is the predominant MAG lipase, were used as the control groups. As shown in Fig. 1a, MAG hydrolase activities were more than 11-fold higher in cancerous lung tissues than in paired non-cancerous tissues. Increased MAG hydrolysis was associated with decreased levels of C16:0 MAG (39.9%) and C18:1 MAG (68.1%) in cancerous versus non-cancerous samples (Fig. 1b). The tissue content of 2-AG was also decreased by 49.0%, but the difference did not reach statistical significance (Fig. 1b).

Previous studies reported that, in different cell systems, overall MAG hydrolysis is primarily mediated by MAGL or ABHD6. Thus, we assessed the protein abundance of MAGL and ABHD6 in 206 NSCLC cancerous tissues and 102 matched adjacent non-cancerous tissues. The expression of ABHD6, but not MAGL, was substantially elevated in NSCLC tissues when compared with adjacent non-cancerous tissues (Fig. 1c–f). The specificity of IHC analysis was evaluated with positive controls of rat brain tissues (Fig. S1a) [14]. Next, we correlated ABHD6 expression with clinicopathological characteristics in this cohort of NSCLC patients (Detailed characteristics of patients are provided in Table S1). High ABHD6 expression was significantly associated with higher TNM stage (P = 0.027) and histological type (P = 0.002) (Table 1). The overall survival was gradually reduced with increasing ABHD6 levels, whereas there was no significant association with MAGL expression (Fig. 1g-h). Further univariate analysis showed that ABHD6 expression (HR, 1.788; P = 0.001), differentiation (HR, 1.441; P = 0.007), lymph node metastasis (HR, 1.423; P = 0.001), and TNM stage (HR, 1.470; $P < 0.001$) were associated with poor overall survival (Table 2). In multivariate analysis, high ABHD6 expression (HR, 1.648; P = 0.007), low differentiation (HR, 1.505; P = 0.004) and advanced TNM stage (HR, 1.382; P = 0.004) had a worse prognosis in NSCLC patients (Table 2). These data indicated that enhanced MAG hydrolase activity and increased ABHD6 protein content are important markers for the prognosis of NSCLC.

3.2. ABHD6 is the primary MAG lipase in NSCLC

To validate the importance of ABHD6 for MAG hydrolase activity of NSCLC, we assessed the protein abundance and enzyme activity of known MAG lipases in a set of NSCLC cell lines and proper control samples. MAGL and ABHD12 were expressed at low level in all NSCLC cell lines and selective inhibition of MAGL by JZL184 did not decrease MAG hydrolase activity of NSCLC cell lysates (Fig. 2a, b and S1b). However, ABHD6 protein abundance was higher in NSCLC cell lines and pancreatic β cells (INS) (Fig. 2a). This is confirmed by immunofluorescence study showing little signal for MAGL, whereas ABHD6 is mainly localized in the cytoplasm of NSCLC cells (Fig. S1c). Using C16:0 MAG as substrate, the addition of the selective ABHD6 inhibitor WWL70 or KT203 significantly decreased cellular MAG hydrolase activities in SPC-A-1 (92.2% and 96.1%) and A549 (89.0% and 94.3%) cell extracts, respectively (Fig. 2b). C18:1 MAG hydrolase activity was also repressed by WWL70 or KT203 treatment in SPC-A-1 (74.7% and 77.4%) and A549 (80.7% and 81.0%) cell extracts (Fig. 2b). Similar to pharmacological inhibition, transient silencing of ABHD6, not MAGL or ABHD12, largely impaired cellular C16:0 MAG hydrolase activity (by 87.5% and 86.5%) and C18:1 MAG hydrolase activity (by 68.4% and 78.6%) in SPC-A-1 and A549 cell extracts (Fig. 2c). Thus, ABHD6 acts as the primary MAG lipase in NSCLC.

3.3. ABHD6 blockade limits cancer aggressiveness of NSCLC

To investigate if increased ABHD6 activity affects the pathophysiology of NSCLC, we inhibited ABHD6 activity with pharmacological blockade (WWL70 or KT203) or shRNA mediated knockdown of ABHD6 (shABHD6) protein expression. Pharmacological or genetic inhibition of ABHD6 significantly limited the invasion and migration of four independent NSCLC cell lines without consistent effects on proliferation rates (Fig. 2d–g, Fig. S1d–S1i). In contrast, pharmacological blockade of MAGL did not alter invasion or migration (Fig. S2a and S2b), suggesting that ABHD6 but not MAGL affects the aggressiveness of NSCLC. To validate these findings in vivo, we subcutaneously injected shControl or shABHD6 NSCLC cells into nude mice and monitored tumor growth. Silencing of ABHD6 significantly delayed tumor growth of NSCLC as compared to controls (Fig. 3a and S2c). To assess metastatic seeding, we also injected shControl or shABHD6 NSCLC cells intravenously. ABHD6 silencing markedly decreased the ability of SPC-A-1 and A549 to seed the lungs by 78.4% and 70.4%, respectively (Fig. 3b and S2d). In a short-term lung metastasis assay, ABHD6 blockade significantly reduced the number of NSCLC cells to seed the lungs without affecting the proliferation of NSCLC cells within metastatic sites (Fig. S2e–S2h), suggesting that the pro-oncogenic role of ABHD6 is primarily mediated via increased cancer aggressiveness.

Considered the pivotal role of epithelial-to-mesenchymal transition (EMT) in determining invasive, migratory, and metastatic capabilities of cancer cells, we examined whether ABHD6 promotes NSCLC via regulating EMT. The protein levels of mesenchymal markers (Vimentin, S100A4, and Snail) were decreased while epithelial marker (E-cadherin) increased upon knockdown of ABHD6 in NSCLC cells (Fig. S3a), suggesting reversal of EMT toward a reduced mesenchymal phenotype. Immunohistochemical staining of tumors derived from NSCLC cells corroborated this finding showing that knockdown of ABHD6 drastically impaired EMT also in vivo (Fig. S3b).

3.4. Overexpression of ABHD6 increases the pathogenic properties of NSCLC

Since ABHD6 blockade significantly reduced the migration, invasion, and in vivo tumor growth of NSCLC, we next examined whether forced overexpression of ABHD6 would provoke the pathogenic potential of NSCLC cells. We stably expressed ABHD6 in H1650 and H1975 cells (Fig. 3c), which exhibit low endogenous ABHD6 levels as compared with other NSCLC cell lines (Fig. 2a). ABHD6-overexpressing (ABHD6-OE)

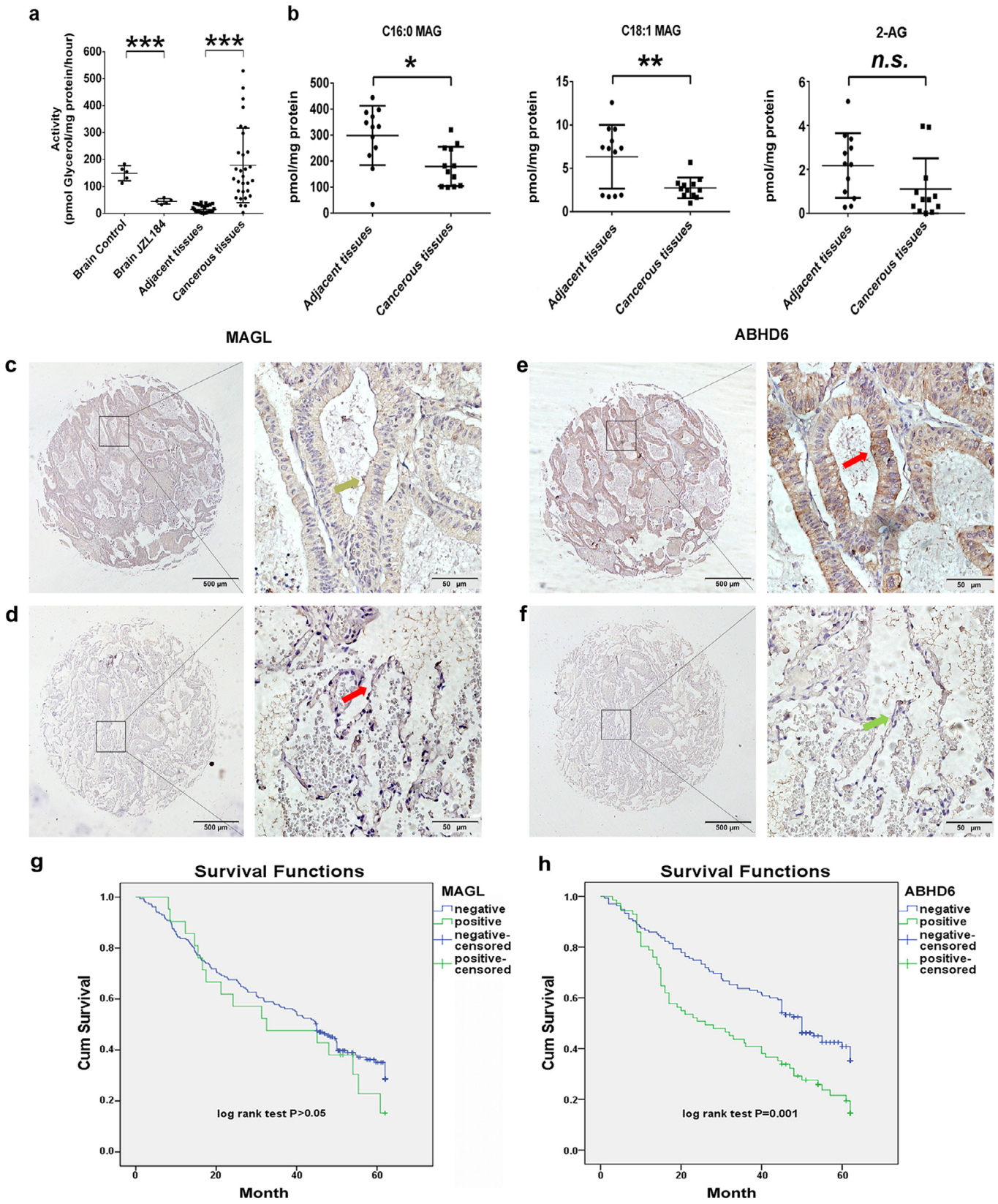

Fig. 1. High ABHD6 expression correlates positively with poor prognosis of NSCLC, where MAG catabolism is elevated in human cancerous lung tissues. a) MAG hydrolase activity in rat brain tissues, human cancerous tissues, and matched adjacent non-cancerous tissues. n = 30/group. $^{***}P < 0.001$ (Student's t-test) versus adjacent tissues. b) Concentrations of MAG species in cancerous tissues and matched adjacent non-cancerous tissues. n = 12/group. $^{*}P < 0.05$; $^{**}P < 0.01$ (Student's t-test) versus adjacent tissues. c, d) Representative images of IHC for MAGL in carcinoma tissues (c) and matched adjacent non-cancerous tissues (d) derived from NSCLC patients. e, f) Representative images of immunohistochemical staining for ABHD6 in carcinoma tissues (e) and matched adjacent non-cancerous tissues (f) derived from NSCLC patients. The left panel of c, d, e, and f are × 40 magnification (bar = 500 μm), and the right panel are × 400 magnification (bar = 50 μm). Strong positive protein expression is indicated by red arrows, weak positive protein expression is indicated by yellow arrows, and negative protein expression is indicated by green arrows. g, h) Kaplan-Meier survival curves of MAGL g) and ABHD6 h) expressions associated with the overall survival rate of NSCLC patients. Data are presented as means ± SD.

Table 1
Correlation of ABHD6 expression in tumorous tissues with clinicopathologic characteristics in NSCLC patients.

Groups	n	ABHD6 expression High (%)	Pearson χ^2	*P* value
Total	206	71(34.47)		
Age				
<60	69	27(39.13)	0.999	0.317
≥60	137	44(32.17)		
Gender				
Female	49	23(46.94)	4.428	0.035*
Male	157	48(30.57)		
Differentiation				
High	31	11(35.49)	1.190	0.552
Middle	113	42(37.17)		
Low	62	18(29.03)		
Histological type				
Adenocarcinoma	59	30(50.85)	12.855	0.002*
Squamous cell carcinoma	96	22(22.92)		
Adenosquamous carcinoma	51	19(37.25)		
T				
Tis + T1	69	26(37.68)	1.160	0.560
T2a	87	27(31.03)		
T2b + T3 + T4	46	18(39.13)		
Unknown	4	0		
N				
N0	111	33(29.73)	2.582	0.275
N1	55	23(41.82)		
N2	40	15(37.50)		
TNM stage				
0–I	81	20(24.69)	7.241	0.027*
II	73	33(45.21)		
III–IV	48	18(37.50)		
Unknown	4	0		

* $P<0.05$.

H1650 and H1975 cells displayed an 82.1% and 42.9% higher invasion rate and a 15.7% and 57.7% higher migration rate than cells transfected with control vectors (Fig. 3d and e). Additionally, ABHD6-OE NSCLC cells exhibited increased tumor growth rates when injected into nude mice (Fig. 3f and S3c). Forced overexpression of ABHD6 also markedly increased the ability of H1650 and H1975 to seed the lungs by 142.9% and 216.7%, respectively (Fig. 3g and S3d). Taken together, these results suggest that increased ABHD6 expression promotes NSCLC.

3.5. Endocannabinoid signaling contributes little to ABHD6 involved pathophysiology of NSCLC

ABHD6 is originally recognized for its role in controlling the cellular abundance of 2-AG, which activates the cannabinoid receptors (CBs) [14]. We therefore treated shControl and shABHD6 NSCLC cells with selective CB1 and CB2 receptor antagonists (50 nM AM251 and 50 nM AM630, respectively). Although AM630 failed in rescuing the invasive and migratory defects of shABHD6 NSCLC cells, partial reversal was observed with AM251 treatment (Fig. S4a-S4d). However, AM251 also non-significantly increases the invasion and migration of shControl NSCLC cells. Our quantitative lipid analysis also illustrated that ABHD6 silencing did not affect intracellular levels of AA or 2-AG (Fig. S5a and S5b), suggesting that the endocannabinoid pathway was not affected by ABHD6 blockade in NSCLC cells. To consolidate this conclusion, we treated shABHD6 NSCLC cells with exogenous AA. AA had little effect on the invasive and migratory capabilities of both shControl and shABHD6 NSCLC cells (Fig. S5c and S5d). Consistent with this finding, AA feeding did not affect tumor growth of SPC-A1 or A549 bearing mice (Fig. S5e and S5f). Additionally, we carefully examined whether ABHD6 inhibition alters intracellular levels of phospholipids and lysophospholipids in NSCLC cells. ABHD6 inhibition did not alter total levels of phospholipids and lysophospholipids in SPC-A1 and A549 cells, despite certain species of phosphatidylcholine, lysophosphatidic acid, and lysophosphatidylcholine did modestly change in A549 cells (Fig. S5g and Table S3).

3.6. Dysregulated MAG substrates impair the pathophysiology of NSCLC

Although the first description of ABHD6 activity highlights its regulation on 2-AG efficacy, ABHD6 also degrades many other MAGs esterified with saturated and monounsaturated FAs [11]. In two NSCLC cell lines we examined, ABHD6 blockade caused significant elevations in intracellular C16:0 MAG and C18:1 MAG levels and corresponding reductions in FA species (Fig. 4a and b). In cancer cells from multiple tissues of origin, MAGL inhibition also led to similar metabolic dysregulations and impaired cancer aggressiveness, which were rescued by exogenous FAs treatment [5,7]. Thus, we examined whether the pathophysiology of NSCLC cells is also affected by exogenous FAs or MAGs. 1 μM C16:0 FA or C18:1 FA supplementation did not affect the migration of shABHD6 NSCLC cells (Fig. 4c), whereas incubation with 1 μM C16:0 MAG or C18:1 MAG significantly increased intracellular MAG concentrations and inhibited the migration of shControl SPC-A-1 and shControl A549 cells (Fig. 4d and e). Moreover, the incubation with 1 μM C16:0 MAG or C18:1 MAG did not alter the migration of shABHD6 NSCLC cells (Fig. 4d). We speculated that high endogenous MAG levels in shABHD6 NSCLC cells may cause migration rates that cannot be further increased by additional supplementation of exogenous MAGs. In line with impaired aggressiveness, epithelial markers were significantly increased while

Table 2
Univariate and multivariable analysis of prognostic factors in NSCLC for 5-year survival.

Varible	Univariate analysis			Multivariate analysis		
	HR	*P*	95%CI	HR	*P*	95%CI
ABHD6 expression High vs low	1.788	0.001*	1.258–2.541	1.648	0.007*	1.148–2.366
Age (years) ≤60 vs >60	0.997	0.986	0.694–1.432			
Gender Male vs female	0.905	0.620	0.609–1.344			
Differentiation Well and moderate vs poor	1.441	0.007*	1.105–1.879	1.505	0.004*	1.144–1.981
Histological type Sq vs Ad vs others	0.847	0.174	0.666–1.076			
T Tis + T1 vs T2a vs T2b + T3 + T4	1.176	0.173	0.932–1.483			
N N0 vs N1 vs N2	1.423	0.001*	1.157–1.752			
TNM stage 0-Ivs II vs III-IV	1.470	<0.001*	1.185–1.823	1.382	0.004*	1.108–1.724

* $P < 0.05$. TNM stage contains N stage, therefore, it was not included in the multivariate analysis.

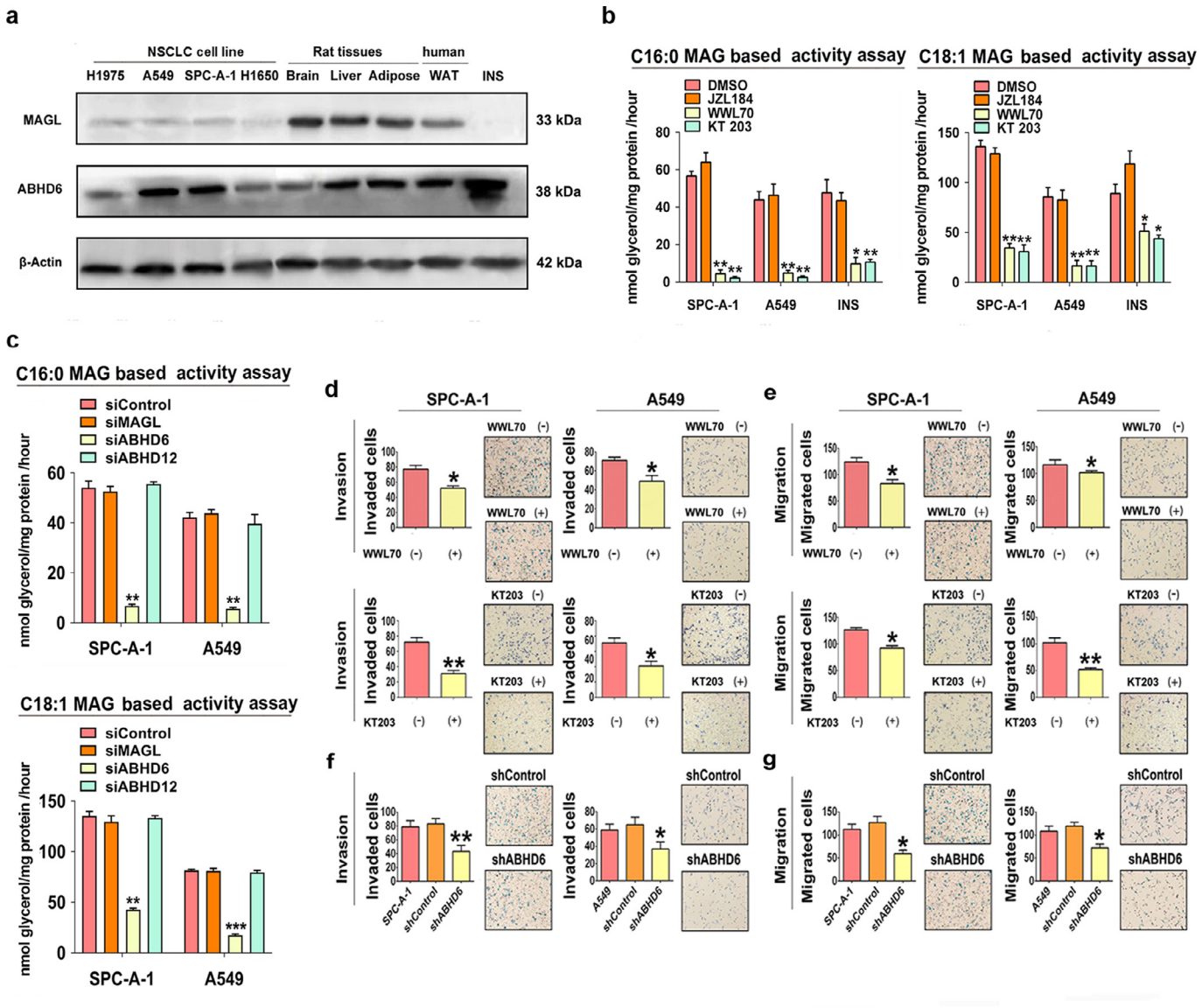

Fig. 2. ABHD6 is the predominant MAG lipase and associated with the aggressive phenotype of NSCLC cells. a) Protein levels of MAGL and ABHD6 in NSCLC cell lines, rat tissues, human white adipose tissue (WAT), and rat insulin secreting β cell (INS). n = 3/group. b) Assessment of MAG hydrolysis using C16:0-MAG (100 μM) or C18:1-MAG (100 μM) as substrate with or without 10 μM WWL70 or 1 μM JZL184 or 10 nM KT203 in SPC-A-1, A549, and INS cells. c) Assessment of MAG hydrolysis using siRNA to knockdown ABHD6, MAGL, or ABHD12 in NSCLC cells. n = 3/group. $^{*}P < 0.05$; $^{**}P < 0.01$; $^{***}P < 0.001$ (one-way ANOVA test) versus Control group. d, e) Invasion d) and migration e) of SPC-A-1 and A549 cells with or without WWL70 or KT203 treatment. n = 5/group. $^{*}P < 0.05$; $^{**}P < 0.01$ (Student's t-test) versus parental group. Technical replicate with n = 3. f, g) Invasion f) and migration g) of shControl, shABHD6, parental SPC-A-1 and A549 cells. n = 5/group. $^{*}P < 0.05$; $^{**}P < 0.01$ (one-way ANOVA test) versus shControl group. Technical replicate with n = 3. Data are presented as means ± SD.

mesenchymal markers were decreased after exposure of NSCLC cells to either C16:0 MAG or C18:1 MAG (Fig. S6a). Together, these findings suggest that elevations of intracellular MAG, either by ABHD6-deficiency or exogenous supplementation limit cancer aggressiveness and associated EMT signaling.

3.7. PPARα/γ links ABHD6-derived signaling lipids to cancer pathophysiology

Recent studies indicated that certain MAG species might serve as PPARs ligands [15,16], and these nuclear receptor transcription factors play pivotal roles on malignancy [20,21]. Our transactivation experiments revealed that the addition of exogenous C16:0 MAG and C18:1 MAG increases PPARα/γ-driven luciferase gene expression in a reporter assay based on HEK293T cell (Fig. S6b). Supplementation with exogenous C16:0 MAG or C18:1 MAG also increased the mRNA expression of PPARα/γ target genes in NSCLC cell lines (Fig. 5a and b). Additionally, the mRNA expression of PPARα/γ target genes was elevated in shABHD6 as compared to shControl NSCLC cell lines (Fig. S6c and S6d).

To investigate if augmented PPAR signaling contributes to the impaired aggressiveness of shABHD6 NSCLC cells, we applied specific PPAR antagonists to the medium of NSCLC cells. Exposure of NSCLC cells to the PPARα antagonist GW6471 increased migration and invasion in shABHD6 but not shControl cells (Fig. 5c and d). Pharmacological antagonism of PPARγ by T0070907 also partly increased indices of aggressiveness in shABHD6 but not shControl NSCLC cells (Fig. 5c and d). Consistently, PPARα/γ antagonism suppressed the elevated PPARα/γ target gene expression and partially rescued the impaired EMT pathway in shABHD6 NSCLC cells, but had no significant effect on shControl cells (Fig. S6c-S6e). Daily treatment of tumor bearing mice with either PPARα or PPARγ antagonists increased tumor

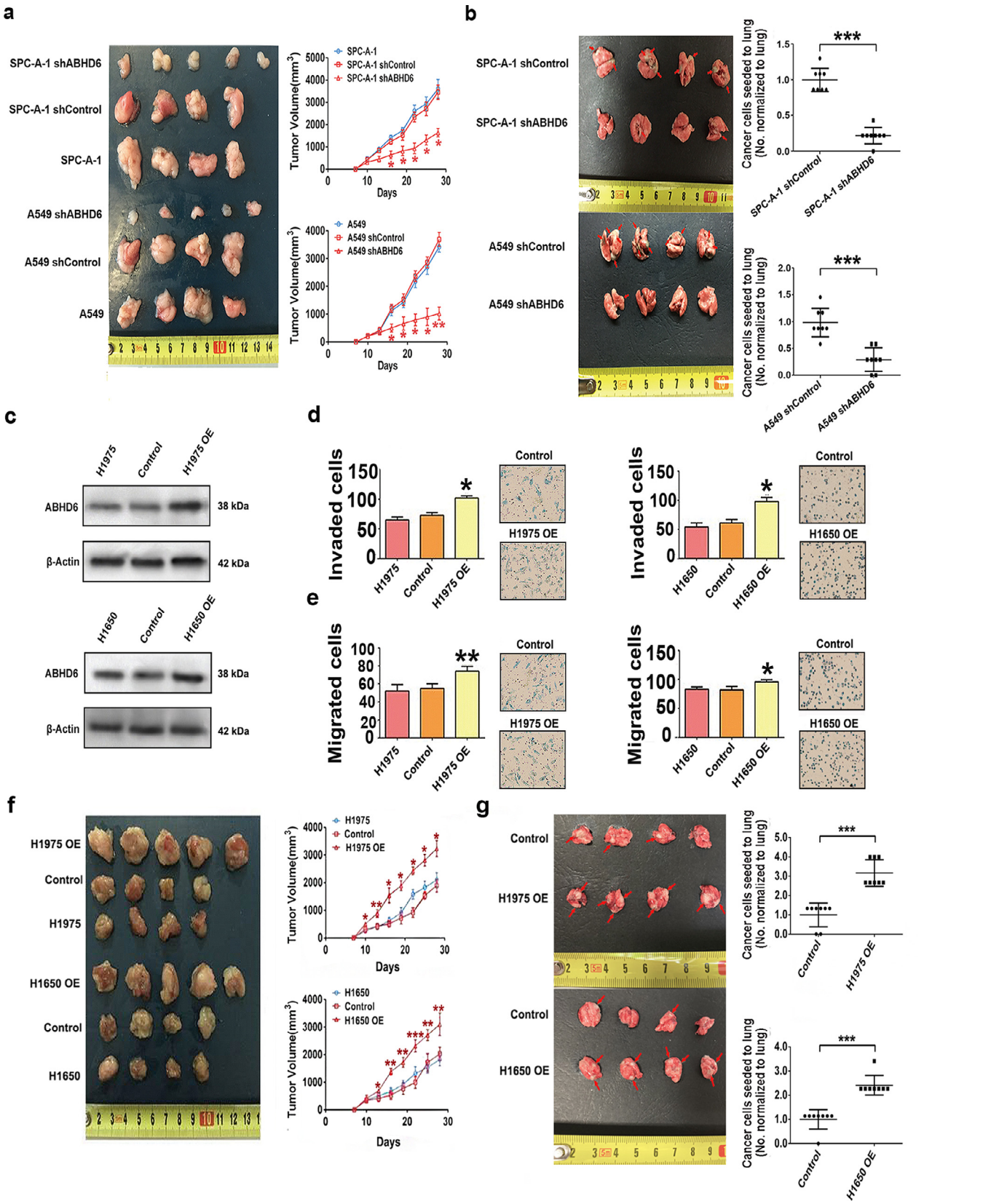

Fig. 3. Alteration in the expression of ABHD6 affect the development of NSCLC. a) Tumor growth after subcutaneous injection with shControl, shABHD6, and parental SPC-A-1 and A549 cells. $n = 4–5$/group. $^{*}P < 0.05$; $^{**}P < 0.01$ (one-way ANOVA test) versus shControl group. b) Metastatic seeding to the lung of shControl/shABHD6 SPC-A-1 and A549 cells 7 weeks after intravenous transplantation. Red arrows indicate cancer cell seeding. $n = 8$/group. $^{***}P < 0.001$ (Student's t-test) versus shControl group. c) Protein levels of ABHD6 in Control, ABHD6-OE, and parental H1650 and H1975 cells. Technical replicate with $n = 3$. d, e) Invasion d) and migration e) of Control, ABHD6-OE, and parental H1975 and H1650 cells. $n = 5$/group. $^{*}P < 0.05$; $^{**}P < 0.01$ (one-way ANOVA test) versus Control group. Technical replicate with $n = 3$. f) Tumor growth after subcutaneous injection with Control, ABHD6-OE, and parental H1975 and H1650 cells. $n = 4–5$/group. $^{*}P < 0.05$; $^{**}P < 0.01$; $^{***}P < 0.001$ (one-way ANOVA test) versus Control group. g) Metastatic seeding to the lung of Control/ABHD6-OE SPC-A-1 and A549 cells 7 weeks after intravenous transplantation. $n = 4–5$/group. $^{***}P < 0.001$ (Student's t-test) versus Control group. Data are presented as means ± SD.

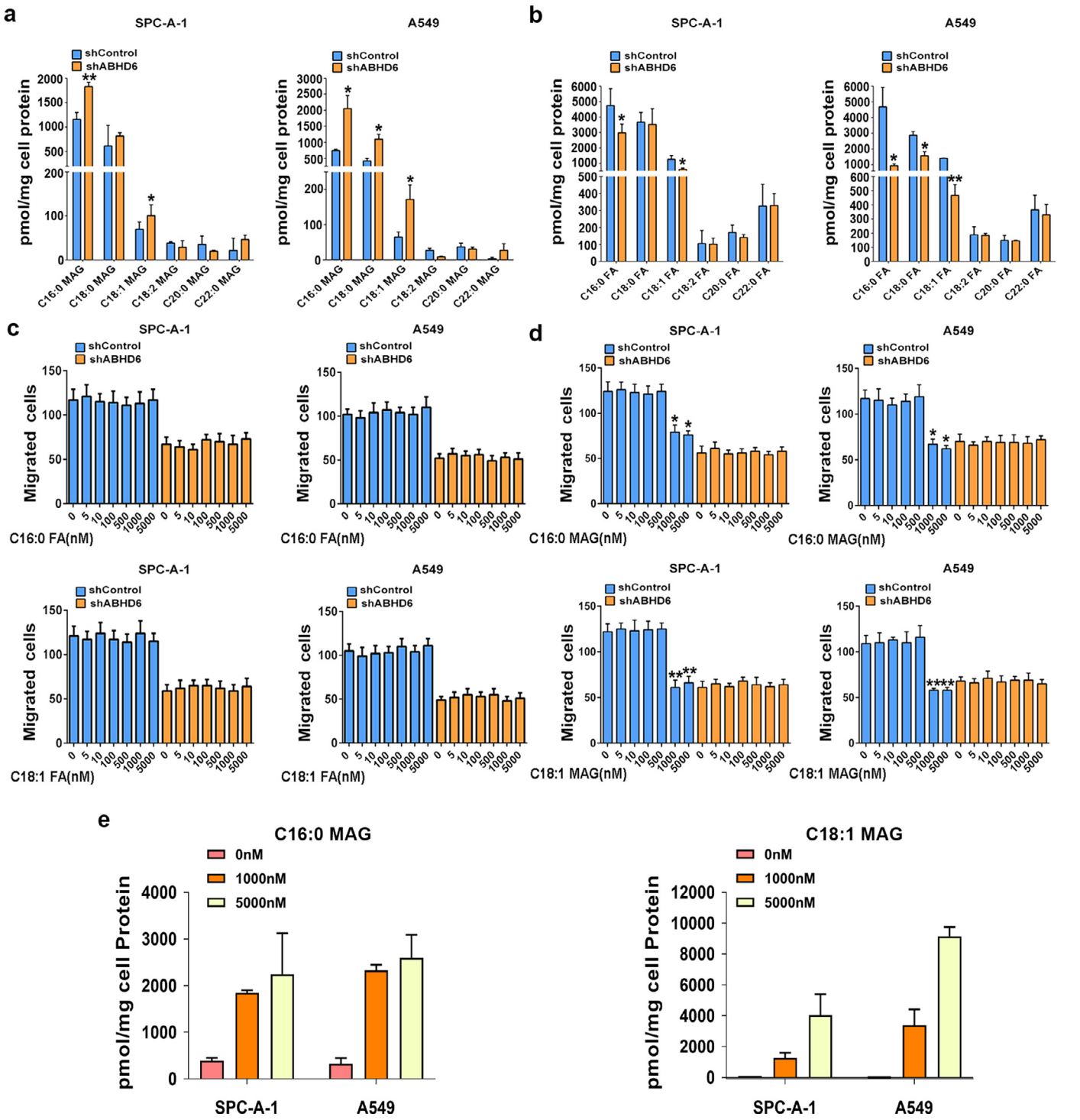

Fig. 4. Dysregulated MAG substrates underlie the pathophysiology of NSCLC a) Intracellular levels of MAG species in shControl/shABHD6 SPC-A-1 and A549 cells. b) Intracellular levels of FA species in shControl/shABHD6 SPC-A-1 and A549 cells. n = 5/group. $^{*}P < 0.05$; $^{**}P < 0.01$ (Student's t-test) versus shControl group. c and d) Migration of shControl/shABHD6 SPC-A-1 and A549 cells with or without FAs c) or MAGs d) treatment. n = 5/group. $^{*}P < 0.05$; $^{**}P < 0.01$ (Student's t-test) versus shControl group without FAs treatment. e) Intracellular levels of C16:0 MAG or C18:1 MAG after exogenous treatment for 8 h. Technical replicate with n = 3. Data are presented as means ± SD.

growth of shABHD6 NSCLC cell lines (Fig. 5e, f and S6f). Notably, combined treatment with PPARα and PPARγ antagonists largely restored the growth of shABHD6 tumors to the rate of shControl tumors. These findings suggest that genetic inhibition of ABHD6 limits NSCLC at least in a large part by PPARα/γ activation via accumulation of excessive MAG.

4. Discussion

The long-term survival of lung cancer is dismal with a 5-year survival rate of around 18% because approximately 75% of these are metastatic, or advanced, at diagnosis [10,22]. Thus, diagnostic and prognostic biomarkers as well as novel therapeutic approaches are urgently needed for prevention and treatment of NSCLC. Since

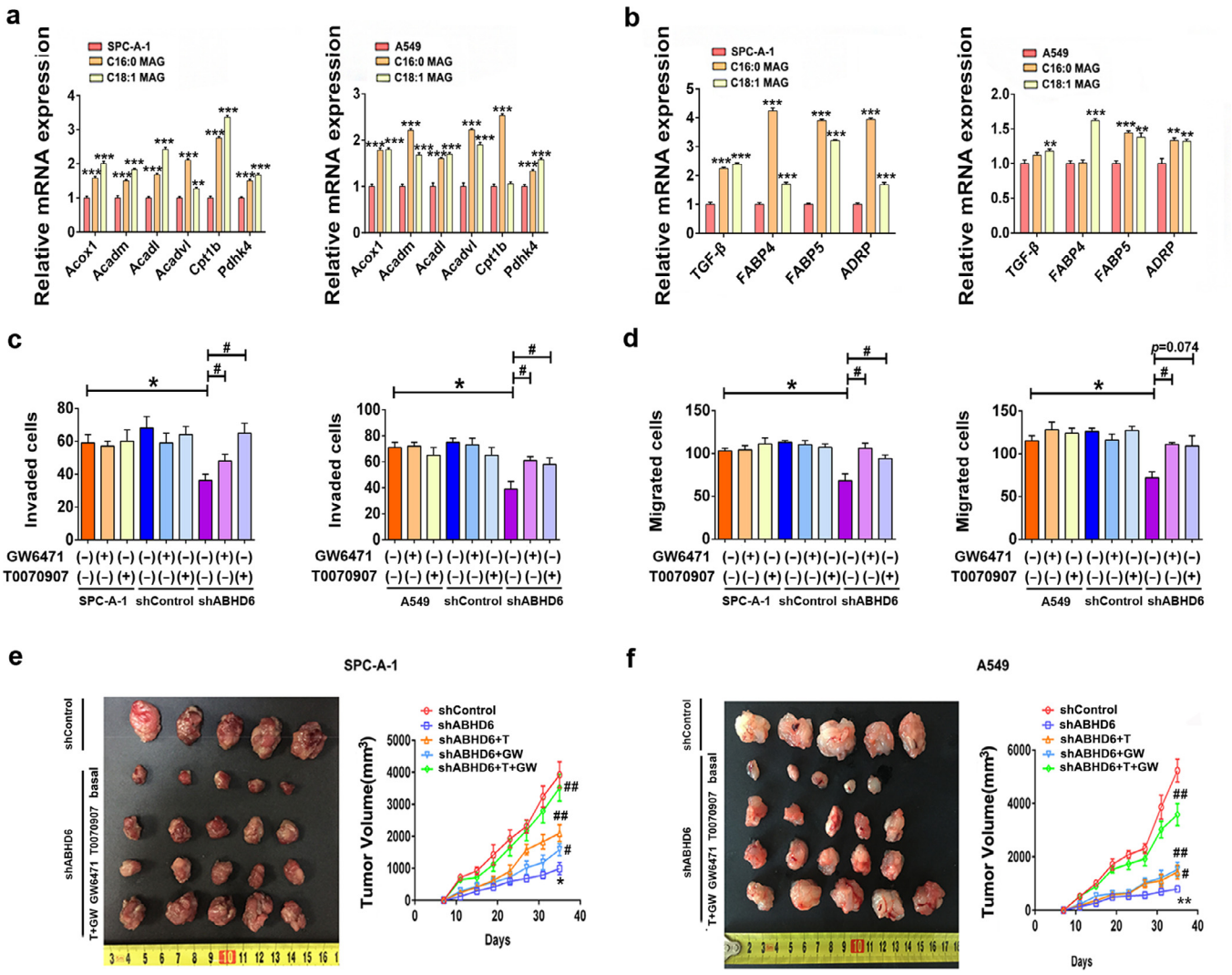

Fig. 5. Accumulated MAGs activate PPARα/γ signaling. a, b) Expressions of PPARα a) and PPARγ b) target genes after MAGs treatment in SPC-A-1 and A549 cells. n = 5/group. $^{*}P < 0.05$; $^{**}P < 0.01$; $^{***}P < 0.001$ (one-way ANOVA test) versus parental group. Technical replicate with n = 3. (c, d) ABHD6 blockade limits the invasion c) and migration d) which can be rescued by 1 μM GW6471 and 1 μM T0070907 treatments in SPC-A-1 and A549 cells. n = 5/group. $^{*}P < 0.05$ (one-way ANOVA test) versus shControl group. $^{\#}P < 0.05$ (one-way ANOVA test) versus shABHD6 group. Technical replicate with n = 3. e, f) ABHD6 blockade impairs the tumor growth, which can be rescued by GW6471 (1 mg/kg body weight) and T0070907 (1 mg/kg body weight) treatments in SPC-A-1 e) and A549 cells f). n = 5/group. $^{*}P < 0.05$, $^{**}P < 0.01$ (one-way ANOVA test) versus shControl group. $^{\#}P < 0.05$; $^{\#\#}P < 0.01$ (one-way ANOVA test) versus shABHD6 group. Data are presented as means ± SD.

the first report on the pro-oncogenic role of MAGL, increasing evidence supports the concept that MAG lipolysis and its downstream signaling play pivotal roles in various kinds of cancers [23]. This raises the question of why evidence is absent for the pro-oncogenic role of MAGL in certain types of cancer, like NSCLC [23].

The present study provides evidence that ABHD6 is the primary MAG lipase and an important oncogene in NSCLC. Pharmacological or genetic blockade of ABHD6 impaired MAG catabolism in NSCLC cells and corrected hallmarks of malignancy. NSCLC patients with concurrent high ABHD6 protein abundance in tumor tissue had poorer prognosis and significantly shorter survival time than patients with low ABHD6 protein levels. Accordingly, a genome-wide association study identified a single nucleotide polymorphism in ABHD6 region is associated with the risk of developing tobacco induced NSCLC [24]. During the course of our work, a pharmacological study identified the ABHD6 inhibitor JCP-265 as an anti-metastatic candidate for pancreatic ductal adenocarcinoma, supporting the potential pro-oncogenic role of ABHD6 in certain types of cancer [25].

Previous studies have shown that ABHD6 acts as the predominant MAG hydrolase in cells with low or absent MAGL expression such as pancreatic β cells and macrophages [12,15]. Moreover, it was suggested that MAGL and ABHD6 differ in subcellular localization and substrate specificity and thus may target different intracellular MAG pools [14,16]. It is therefore conceivable that differences in expression and subcellular localization account for the differential contribution of both enzymes to MAG hydrolysis of diverse cancers. Nevertheless, these observations foster the view that increased intracellular MAG hydrolysis via either MAGL or ABHD6 is a common metabolic event among top five deadliest cancers, including lung cancer, colorectal cancer, breast cancer, pancreatic cancer, and prostate cancer [5,7,8,25].

ABHD6 was originally described as a MAG hydrolase degrading the endocannabinoid 2-AG [26]. However, our lipid analysis showed little difference in 2-AG or AA levels between shControl and shABHD6 NSCLC cells. These data, in combination with the lack of effect of exogenous AA on NSCLC, argue against the hypothesis that ABHD6 stimulates cancer aggressiveness via excessive catabolism of 2-AG and/or increased eicosanoid synthesis. Besides 2-AG, recent studies suggested that ABHD6's additional ability to hydrolyze a variety of lipid substrates, including phospholipids, lysophospholipids, and bis (monoacylglycerol)phosphate (BMP) [27,28]. However, our lipidomics approach showed nearly unchanged intracellular levels of phospholipids and lysophospholipids between shControl and shABHD6

NSCLC cells, probably due to this activity is only about 5% of its MAG hydrolase activity [29]. Additionally, we examined the lysosomal stability, the proposed downstream of BMP dysregulation, with a specific label for Acridine Orange in shControl/shABHD6 NSCLC cells [28]. However, ABHD6 blockade exhibited little effect on lysosomal stability both, of NSCLC cells (data not shown). Nevertheless, ABHD6's additional hydrolase activities on phospholipids, lysophospholipids, or BMP are independent of MAGL, arguing against a common role of these metabolites in diverse cancer cells associated with increased MAG hydrolysis [28].

Consistent with its primary function as a MAG lipase, we observed increased levels of certain saturated and monounsaturated MAG species upon blocking ABHD6 as well as decreased levels of corresponding FAs in NSCLC cells. Similarly, it has been proposed that MAGL promotes cancer aggressiveness predominantly through its MAG hydrolase activity and the subsequent conversion of FAs towarding an array of oncogenic signature lipids [5,7]. Exogenous FAs treatment (20 μM) could recover the impaired pathophysiology of MAGL disrupted cancer cells [5,7]. However, exogenous sources of FAs failed to rescue impaired migration of shABHD6 cells at a comparable lower dose range (1−5 μM), whereas MAGs significantly reduced the migration of shControl NSCLC cells at the concentration. Since both MAGs and FAs could be taken up by cells, it appears that accumulations of MAGs prefer to decreased FA concentrations largely impair migratory capability of NSCLC cells [15,30,31].

Although the potential role of MAGs were un-recognized in cancer metabolism, current research efforts indicated that intracellular MAGs serve as a "signaling competent pool" beyond endocannabinoid system [23,32]. In pancreatic β cells, C16:0 MAG, C18:0 MAG, and C18:1 MAG are insulinotropic signaling lipids that significantly induce insulin exocytosis [15]. In adipose tissue, it has been demonstrated that ABHD6 silencing induces accumulations of C16:0 MAG and C18:1 MAG to promote the formation of beige adipocytes [16]. Mechanistically, MAGs regulate various physiological and pathological processes via cellular targets such as PPARs, G protein-coupled receptor 119 (GPR119), vanilloid receptor 1 (TRPV1), and mammalian unc13-1 (Munc13-1) [15,16,33,34]. Among them, it has been shown that PPARs activation prevents cancer cells from acquiring invasive and migratory capabilities [20,35]. The activation of PPARα/γ signaling inhibits the Wnt/β-catenin pathway, a key mechanism promoting EMT and metastasis in malignancy [36−38]. In the present study, silencing of ABHD6 led to an induction of PPARα/γ target genes in NSCLC cells. Supplementation with exogenous MAGs elicited a similar transcriptional response and suppressed the malignant signature of NSCLC cells. Of note, PPARα/γ antagonism was sufficient to prevent the suppression of malignant phenotypes that occurred in response to ABHD6 silencing. However, considering that MAG mobilization feeds into a diverse lipid network, it is possible that other signaling molecules and related targets also contribute to pathogenic properties of NSCLC. Additionally, one might also anticipate that ABHD6 affects immune microenvironment of NSCLC, although we should note that the present study was performed in nude mice with an inhibited immune system. Therefore, our findings demonstrate that ABHD6 promotes NSCLC pathogenesis in a cell-autonomous manner.

In summary, the present study shows that intracellular MAG hydrolysis of NSCLC is modulated by ABHD6. High ABHD6 protein content promotes the aggressiveness of NSCLC, causing a poor prognosis. The results also identify that ABHD6-accessible MAG species as previously unappreciated signailling lipids involved in cancer metabolism, which may prove to be of broad significance in various cancer types. Future studies will be required to determine precisely the expression pattern and lipid substrates of MAG lipases in different malignancies.

Declaration of Competing Interest

The authors declare no potential conflicts of interest.

Acknowledgments

We thank the clinical biobank members in Affiliated Hospital of Nantong University.

Funding

This work was supported by the Project for Major New Drug Innovation and Development (2015ZX09501010 and 2018ZX09711001-002-003), Overseas Expertise Introduction Project for Discipline Innovation (G20582017001), European Research Council LipoCheX (grant number 340896), Nantong Science and Technology Plan (HS2018003, MS22018004, MS32017007, and JCZ18109), and Jiangsu Province Clinical Key Research (BE2018670). The funders had no role in study design, data collection, data analysis, interpretation, or writing of the report.

Author Contributions

ZT, HX, JH and JN conceived and performed the experiments and analyzed data. CH, QZ and TE performed the measurement for lipid metabolites and analyzed the data. GS and RZ helped analysis of results and discussion. SN and HH conceived the project, designed the study and analyzed the results. HX, ZT, and HH wrote the manuscript.

Supplementary materials

Supplementary material associated with this article can be found in the online version at doi:10.1016/j.ebiom.2020.102696.

References

[1] Warburg O. On the origin of cancer cells. Science 1956;123(3191):309–14.
[2] Menendez JA, Lupu R. Fatty acid synthase and the lipogenic phenotype in cancer pathogenesis. Nat Rev Cancer 2007;7(10):763–77.
[3] Svensson RU, Shaw RJ. Lipid synthesis is a metabolic liability of non-small cell lung cancer. Cold Spring Harb Symp Quant Biol 2016;81:93–103.
[4] Wise DR, Thompson CB. Glutamine addiction: a new therapeutic target in cancer. Trends Biochem Sci 2010;35(8):427–33.
[5] Nomura DK, Long JZ, Niessen S, Hoover HS, Ng SW, Cravatt BF. Monoacylglycerol lipase regulates a fatty acid network that promotes cancer pathogenesis. Cell 2010;140(1):49–61.
[6] Hu WR, Lian YF, Peng LX, Lei JJ, Deng CC, Xu M, et al. Monoacylglycerol lipase promotes metastases in nasopharyngeal carcinoma. Int J Clin Exp Pathol 2014;7(7):3704–13.
[7] Nomura DK, Lombardi DP, Chang JW, Niessen S, Ward AM, Long JZ, et al. Monoacylglycerol lipase exerts dual control over endocannabinoid and fatty acid pathways to support prostate cancer. Chem Biol 2011;18(7):846–56.
[8] Zhu W, Zhao Y, Zhou J, Wang X, Pan Q, Zhang N, et al. Monoacylglycerol lipase promotes progression of hepatocellular carcinoma via NF-κB-mediated epithelial-mesenchymal transition. J Hematol Oncol 2016;9(1):127.
[9] Matuszak N, Hamtiaux L, Baldeyroux B, Muccioli GG, Poupaert JH, Lansiaux A, et al. Dual inhibition of MAGL and type II topoisomerase by N-phenylmaleimides as a potential strategy to reduce neuroblastoma cell growth. Eur J Pharm Sci 2012;45(3):263–71.
[10] Siegel RL, Miller KD, Jemal A. Cancer statistics, 2018. CA Cancer J Clin 2018;68(1):7–30.
[11] Blankman JL, Simon GM, Cravatt BF. A comprehensive profile of brain enzymes that hydrolyze the endocannabinoid 2-arachidonoylglycerol. Chem Biol 2007;14(12):1347–56.
[12] Alhouayek M, Masquelier J, Cani PD, Lambert DM, Muccioli GG. Implication of the anti-inflammatory bioactive lipid prostaglandin D2-glycerol ester in the control of macrophage activation and inflammation by ABHD6. Proc Natl Acad Sci U S A 2013;110(43):17558–63.
[13] Fisette A, Tobin S, Décarie-Spain L, Bouyakdan K, Peyot ML, Madiraju S, et al. α/β-Hydrolase domain 6 in the ventromedial hypothalamus controls energy metabolism flexibility. Cell Rep 2016;17(5):1217–26.
[14] Marrs WR, Blankman JL, Horne EA, Thomazeau A, Lin YH, Coy J, et al. The serine hydrolase ABHD6 controls the accumulation and efficacy of 2-AG at cannabinoid receptors. Nat Neurosci 2010;13(8):951–7.
[15] Zhao S, Mugabo Y, Iglesias J, Xie L, Delghingaro-Augusto V, Lussier R, et al. α/β-Hydrolase domain-6-accessible monoacylglycerol controls glucose-stimulated insulin secretion. Cell Metab 2014;19(6):993–1007.
[16] Zhao S, Mugabo Y, Ballentine G, Attane C, Iglesias J, Poursharifi P, et al. α/β-Hydrolase domain 6 deletion induces adipose browning and prevents obesity and type 2 diabetes. Cell Rep 2016;14(12):2872–88.

[17] Li F, Fei X, Xu J, Ji C. An unannotated alpha/beta hydrolase superfamily member, ABHD6 differentially expressed among cancer cell lines. Mol Biol Rep 2009;36(4):691–6.
[18] Max D, Hesse M, Volkmer I, Staege MS. High expression of the evolutionarily conserved alpha/beta hydrolase domain containing 6 (ABHD6) in ewing tumors. Cancer Sci 2009;100(12):2383–9.
[19] Shui G, Guan XL, Low CP, Chua GH, Goh JS, Yang H, et al. Toward one step analysis of cellular lipidomes using liquid chromatography coupled with mass spectrometry: application to *Saccharomyces cerevisiae* and *Schizosaccharomyces pombe* lipidomics. Mol Biosyst 2010;6(6):1008–17.
[20] Pozzi A, Capdevila JH. PPARalpha ligands as antitumorigenic and antiangiogenic agents. PPAR Res 2008;2008:906542.
[21] Reddy AT, Lakshmi SP, Reddy RC. PPARγ as a novel therapeutic target in lung cancer. PPAR Res 2016;2016:8972570.
[22] Reade CA, Ganti AK. EGFR targeted therapy in non-small cell lung cancer: potential role of cetuximab. Biologics 2009;3:215–24.
[23] Grabner GF, Zimmermann R, Schicho R, Taschler U. Monoglyceride lipase as a drug target: at the crossroads of arachidonic acid metabolism and endocannabinoid signaling. Pharmacol Ther 2017;175:35–46.
[24] Perez-Gracia JL, Pajares MJ, Andueza MP, Pita G, de Torres Tajes JP, Casanova C, et al. Identification through genome-wide association study (GWAS) of single nucleotide polymorphisms (SNPs) associated with extreme phenotypes of tobacco-induced non-small cell lung cancer (NSCLC) risk. J Clin Oncol 2014;32(15_suppl):11046.
[25] Grüner BM, Schulze CJ, Yang D, Ogasawara D, Dix MM, Rogers ZN, et al. An in vivo multiplexed small-molecule screening platform. Nat Methods 2016;13(10):883–9.
[26] Poursharifi P, Madiraju S, Prentki M. Monoacylglycerol signalling and ABHD6 in health and disease. Diabetes Obes Metab 2017;19(Suppl 1):76–89.
[27] Thomas G, Betters JL, Lord CC, Brown AL, Marshall S, Ferguson D, et al. The serine hydrolase ABHD6 is a critical regulator of the metabolic syndrome. Cell Rep 2013;5(2):508–20.
[28] Pribasnig MA, Mrak I, Grabner GF, Taschler U, Knittelfelder O, Scherz B, et al. α/β Hydrolase domain-containing 6 (ABHD6) degrades the late endosomal/lysosomal lipid bis(monoacylglycero)phosphate. J Biol Chem 2015;290(50):29869–81.
[29] Grabner GF, Fawzy N, Pribasnig MA, Trieb M, Taschler U, Holzer M, et al. Metabolic disease and ABHD6 alter the circulating bis(monoacylglycerol)phosphate profile in mice and humans. J Lipid Res 2019;60(5):1020–31.
[30] Wyllie R, H. J. Pediatric gastrointestinal and liver disease. (4th ed) 2011.
[31] Ho SY, Storch J. Common mechanisms of monoacylglycerol and fatty acid uptake by human intestinal Caco-2 cells. Am J Physiol Cell Physiol 2001;281(4):C1106–17.
[32] Cao JK, Kaplan J, Stella N. ABHD6: its place in endocannabinoid signaling and beyond. Trends Pharmacol Sci 2019;40(4):267–77.
[33] Hansen KB, Rosenkilde MM, Knop FK, Wellner N, Diep TA, Rehfeld JF, et al. 2-Oleoyl glycerol is a GPR119 agonist and signals GLP-1 release in humans. J Clin Endocrinol Metab 2011;96(9):E1409–17.
[34] Iwasaki Y, Saito O, Tanabe M, Inayoshi K, Kobata K, Uno S, et al. Monoacylglycerols activate capsaicin receptor, TRPV1. Lipids 2008;43(6):471–83.
[35] Tachibana K, Yamasaki D, Ishimoto K, Doi T. The role of PPARs in cancer. PPAR Res 2008;2008:102737.
[36] Cheng R, Ding L, He X, Takahashi Y, Ma JX. Interaction of PPARα with the canonic wnt pathway in the regulation of renal fibrosis. Diabetes 2016;65(12):3730–43.
[37] DiMeo TA, Anderson K, Phadke P, Fan C, Perou CM, Naber S, et al. A novel lung metastasis signature links WNT signaling with cancer cell self-renewal and epithelial-mesenchymal transition in basal-like breast cancer. Cancer Res 2009;69(13):5364–73.
[38] Moldes M, Zuo Y, Morrison RF, Silva D, Park BH, Liu J, et al. Peroxisome-proliferator-activated receptor gamma suppresses WNT/beta-catenin signalling during adipogenesis. Biochem J 2003;376(Pt 3):607–13.